Indian Journal of Engineering & Materials Sciences
Vol. 27, February 2020, pp. 33-46

Heat transfer and magneto-hydrodynamic nanofluids flow behaviors past a nonlinear stretching surface considering viscous dissipation and joule heating

Santosh Chaudhary[a*], KM Kanika[b] & Susheela Chaudhary[c]

[a,b]Department of Mathematics, Malaviya National Institute of Technology, Jaipur 302017, India

[c]Department of Mathematics, Government Science College, Sikar 332001, India

Received: 9 July 2019; Accepted: 26 November 2019

Mathematical investigation has been presented to examine the magnetohydrodynamic boundary layer flow of viscous nanofluids bygone a nonlinear stretched plate among cumulative impact of viscous dissipation and joule heating. Physical formulation produced a system of partial differential equations which has been converted into a set of ordinary differential equations through employing suitable similarity variables. For numerical solutions of resulting governing equations of flow, a Keller-box method has been addressed. Results of dimensionless velocity and dimensionless temperature for impacts of various types of nanoparticle along with water base fluid and effects of physical parameters, namely solid volume fraction, nonlinear stretching parameter, magnetic parameter and Brinkmann number have been deliberated *via* graphs. Additionally, surface shear stress and surface heat flux for selected suitable values of pertinent parameters have been computed and explicated *via* table.

Keywords: Heat transfer, Magneto-hydrodynamic, Nanofluids flow, Nonlinear stretching surface, Viscous dissipation, Joule heating

1 Introduction

Heat transfer is a thermal energy action, which corporate with the generation, conversion, and replacement of heat and thermal energy between physical structures. In nature, heat transfer is a boundless circumstance, it occurs along to the temperature difference between medium or within a similar frame. Heat transfer can be classified in different ways like thermal radiation, conduction and convection. There are a lot of applications such as fuel cells, recovery of waste heat, microelectronics, metal metallurgy, nuclear power plant, heat pump in energy, heat employment in solar energy and storage of chemical energy in the area of engineering and industry. A study of unsteady heat transfer flow over convection by the ambient in the turbulent channel is pioneered by Yan[1]. Further, Datta[2] inspected the non-Newtonian fluid flow with heat transfer access tubes. Numerous elaborate and comprehensive explorations such as Khanafer *et al.*[3], Wang and Yang[4], Hong and Asako[5], Yan and Gu[6], Turkyilmazoglu[7] and Chaudhary and Choudhary[8] are addressed the heat transfer properties. Recently, Zhang *et al.*[9] and Afridi and Qasim[10] have conducted the numerical studies of heat transfer flow with various conditions.

Along with a magnetic influence, an analysis of electrically conducting fluids namely liquid metals, salt water and plasmas is known as magneto-hydrodynamic. Magnetic field intensity controls the nature of liquid and can change the heat transfer properties via rearranging fluid concentration. In a fluid, magnetic field consumed current flows that build forces on the fluid. MHD relations developed by the combination of electromagnetism equations of Maxwell and Navier-stokes equations of fluid-mechanics. In the last some decades, the MHD analysis in fluid flow achieved extensive attention in many fields like as physics, chemistry, polymer industry and engineering. MHD is frequently applied in the applications such as walls cooling an inside nuclear reactor, separation of sink-float, metal casting, disease diagnostic processes, fusing metals in an electric furnace, blood pump machines and loudspeakers construction as sealing materials. Hayat *et al.*[11] initiated the analysis of MHD boundary layer flow of an Oldroyd-B fluid. After that, Siddheshwar and Mahabaleswar[12], Abdelkhalek[13], Turkyilmazoglu[14] and Chaudhary and Kumar[15] are

*Corresponding author (E-mail: d11.santosh@yahoo.com)

excellently illustrated the research information extent in the field of MHD flow. In recent years, several researchers like Imtiaz *et al.*[16] and Chaudhary *et al.*[17] explored the MHD flow problems.

Ordinary fluids, specifically water, mineral oils, ethylene glycol and air with suspended nanoparticles mainly made by metals, non-metals, oxides, nitrides and carbides are certified as nanofluids, which have high capabilities for heat transfer and more thermal conductivity than basic fluids. Nanoparticles are taken with a size smaller than 100 nm. The study of nanofluids provides applications in the field of the power plant, manufacturing biomedical and engineering namely solar energy, cancer therapy, systems of energy storage, lubrication technologies, food processing and heat exchangers. Choi[18] is the first one who created the term nanofluid to enlarge the fluid thermal conductivity. Whereas, Eastman *et al.*[19] depicted a study of copper-ethylene glycol nanofluid with increment in effective thermal conductivity. Moreover, Koo and Kleinstreuer[20], Akbarinia[21], Rana *et al.*[22], Moghari *et al.*[23], Sheikholeslami and Rokni[24], and Sheikholeslami and Zeeshan[25] created global literature on fluid flow analysis with the suspended nano-sized solid particles.

The study of fluid flow towards a stretchable sheet is extrusive in crowded industrial and engineering applications. Some cases of applications are drawing of wire, rubber sheet, manufacturing of glass fiber, polymer extrusion via dye, paper cooling and drying, increment in paint efficiency and lubrication, a wind-up roll, copper wires annealing, liquid crystals and filaments. These applications have a considerable contract of research interest along with its bearing. The exploration of boundary layer flow by providing an exact solution for governing equations due to the stretching plate is initiated through Nazar *et al.*[26]. Latterly, Cortell[27] discussed the radiation and heat generation/absorption impact on magnetohydrodynamic flow past a stretching surface. Also, Jat and Chaudhary[28], Cortell[29], Hayat *et al.*[30], Chaudhary and Choudhary[31], and Saadatmandi and Sanatkar[32] presented some articles along with these aspects in fluid flow.

Energy viscous dissipation simplified as an effort executed through velocity across viscous stresses. Until, a substance is known as Joule heating or ohmic heating, if conduction electrons transfer energy to atoms of the conductor by the collision procedure. Eckert number and multiplication of magnetic parameter and Eckert number characterize the viscous dissipation and Joule heating respectively. Viscous dissipation and Joule heating are additional influential for heating or cooling of the plate. Effect of viscous dissipation and Joule heating have vital importance because of their relevance to nuclear engineering and geophysical flow with associated applications such as a drawing of glass fiber and wire, designs of the heat exchanger, a system of power generation, nuclear reactors cooling and liquid metal fluids. Magnetohydrodynamic forced convection in a fluid-brimming permeable surface over a horizontal cylinder along with the influence of viscous dissipation and Joule heating is addressed by El-Amin[33]. Few articles via this direction are established by Abo-Eldahab and El Aziz[34], Jat and Chaudhary[35] and Reddy *et al.*[36]. In the latest, Hussain *et al.*[37] and Chaudhary and Choudhary[38] considered the impacts of viscous dissipation and Joule heating.

An attentive literature survey reveals that there is no investigation available yet which studies the boundary layer flow of nanofluids past the nonlinear stretching surface in the existence of a magnetic field. To fill up this disparity, the main aim of current exploration is to extend the study of Hamad and Ferdows[39]. MHD flow of different types of nanoparticles namely silver (Ag), copper (Cu), titanium dioxide (TiO_2) and aluminum oxide (Al_2O_3) with the base fluid water over to the effects of viscous dissipation and Joule heating are also assumed into consideration. The numerical solution of the problem is attained by using a Keller-box method. Based on the practical application of equipment cooling like telecommunication enclosures, computers and compact power supplies, effort to increase the heat transfer are needed. So the metallic nanoparticles are added into the water because metallic nanoparticles have higher thermal conductivity and rate of heat transfer. This study is illustrated to highlight the impacts of particular values of physical parameters on the nanofluid flow.

2 Mathematical Analysis

Let assume the steady-state, two-dimensional viscous nanofluids flow towards a stretching plate along to the viscous dissipation and Joule heating impact. The coordinate system (x, y) identifies in Fig. 1 that $x-$direction is taken parallel to the wall and $y-$direction is taken normal to the wall. The

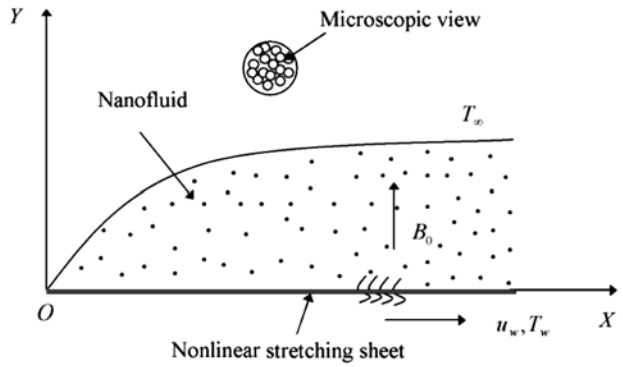

Fig. 1 — Flow configuration and coordinate system.

plate is considered at $x-$ axis and it is stretched with the non-linear velocity $u_w = cx^n$ at the temperature $T_w = T_\infty + bx^{2n}$, where b, c are positive constants, n is the nonlinear stretching parameter and T_∞ is the ambient fluid temperature. Keeping in the view of thermal equilibrium, there is no slip occurs between the ordinary fluid and the suspended nanoparticles. It is also surmised that fluid is electrically conducting, thus the Lorentz force $\vec{J} \times \vec{B}$ condition included in the momentum equation, where $\vec{J}$ is the electrical current density, $\vec{B} = (0, B_0, 0)$ is the transverse magnetic field and B_0 is the magnetic field applied perpendicular to the plate. A small value of magnetic Reynolds number is enough to show that the influence of the induced magnetic field can be neglected. Following governing equation are obtained by using the above assumptions as (Bansal[40]) :

$$\frac{\partial u}{\partial x} + \frac{\partial v}{\partial y} = 0 \qquad \text{... (1)}$$

$$u\frac{\partial u}{\partial x} + v\frac{\partial u}{\partial y} = \upsilon_{nf}\frac{\partial^2 u}{\partial y^2} - \frac{(\sigma_e)_{nf} B_0^{\,2}}{\rho_{nf}} u \qquad \text{... (2)}$$

$$u\frac{\partial T}{\partial x} + v\frac{\partial T}{\partial y} = \alpha_{nf}\frac{\partial^2 T}{\partial y^2} + \frac{\mu_{nf}}{(\rho C_p)_{nf}}\left(\frac{\partial u}{\partial y}\right)^2 + \frac{(\sigma_e)_{nf} B_0^{\,2}}{(\rho C_p)_{nf}} u^2 \qquad \text{... (3)}$$

along to the associated boundary conditions,

$$\begin{aligned} &y = 0: \quad u = u_w,\ v = 0,\ \ T = T_w \\ &y \to \infty: \quad u \to 0,\ T \to T_\infty \end{aligned} \qquad \text{... (4)}$$

where subscript nf denotes the nanofluid properties, u and v are the velocity components corresponding to the $x-$ and $y-$axes respectively, $\upsilon = \frac{\mu}{\rho}$ is the kinematic viscosity, μ is the coefficient of viscosity, ρ is the density, σ_e is the electrical conductivity, T is the temperature of nanofluid, $\alpha = \frac{\kappa}{\rho C_p}$ is the thermal diffusivity, κ is the thermal conductivity and C_p is the specific heat at constant pressure.

Further, physical characteristics of nanofluid namely coefficient of viscosity, density, electrical conductivity, thermal conductivity and heat capacitance for spherical shaped nanoparticles continued from Mohyud-Din *et al.*[41] are given as follows

$$\mu_{nf} = \frac{\mu_f}{(1-\phi)^{5/2}} \qquad \text{... (5)}$$

$$\rho_{nf} = (1-\phi)\rho_f + \phi\rho_s \qquad \text{... (6)}$$

$$(\sigma_e)_{nf} = (\sigma_e)_f - \frac{3\phi[(\sigma_e)_f - (\sigma_e)_s]}{2(\sigma_e)_f + (\sigma_e)_s + \phi[(\sigma_e)_f - (\sigma_e)_s]}(\sigma_e)_f \qquad \text{... (7)}$$

$$\kappa_{nf} = \kappa_f - \frac{3\phi(\kappa_f - \kappa_s)}{2\kappa_f + \kappa_s + \phi(\kappa_f - \kappa_s)}\kappa_f \qquad \text{... (8)}$$

$$(\rho C_p)_{nf} = (1-\phi)(\rho C_p)_f + \phi(\rho C_p)_s \qquad \text{... (9)}$$

where subscripts f and s indicate the physical properties for base fluid and nano solid particles, respectively and ϕ is the solid volume fraction. Moreover, values of thermophysical properties of nanoparticles and base fluid are introduced in Table 1 (Su and Zheng[42]).

3 Similarity Transformation

To solve the governing Eqs. (1) to (3), a stream

Table 1 — Thermophysical properties of used materials in present study.

Properties	Ag	Cu	TiO_2	Al_2O_3	Water
$\kappa(Wm^{-1}K^{-1})$	429	400	8.9538	40	0.613
$\rho\,(Kgm^{-3})$	10500	8933	4250	3970	997.1
$C_p\,(JKg^{-1}K^{-1})$	235	385	686.2	765	4179
$\sigma_e(Sm^{-1})$	6.3×10^7	5.96×10^7	0.24×10^7	3.69×10^7	0.05

function $\psi(x,y)$ is defined in the usual way that $u=\frac{\partial\psi}{\partial y}$ and $v=-\frac{\partial\psi}{\partial x}$, which symmetrically satisfies the continuity Eq. (1), similarity variable η and the non-dimensional temperature $\theta(\eta)$ are taken to followed as Hamad and Ferdows[39] in the following structure

$$\psi=\left(\frac{2c\upsilon_f}{n+1}\right)^{1/2}x^{\frac{n+1}{2}}f(\eta),$$

$$\eta=\left[\frac{c(n+1)}{2\upsilon_f}\right]^{1/2}x^{\frac{n-1}{2}}y,\quad T=T_\infty+(T_w-T_\infty)\theta(\eta) \qquad \text{... (10)}$$

where $f(\eta)$ is the dimensionless stream function.

After imposing the similarity transformations Eq. (10), the governing boundary layer Eqs. (2) and (3) corresponding to the boundary conditions Eq. (4) are modified as follows

$$f'''+(1-\phi)^{5/2}\left(1-\phi+\phi\frac{\rho_s}{\rho_f}\right)\left(ff''-\frac{2n}{n+1}f'^2\right)-2(1-\phi)^{5/2}\frac{(\sigma_e)_{nf}}{(\sigma_e)_f}\frac{M}{(n+1)}f'=0 \qquad \text{... (11)}$$

$$\frac{\kappa_{nf}}{\kappa_f}\theta''+\left[1-\phi+\phi\frac{(\rho C_p)_s}{(\rho C_p)_f}\right]Pr\left(f\theta'-\frac{4n}{n+1}f'\theta\right)+\frac{1}{(1-\phi)^{5/2}}Br\left[f''^2+2(1-\phi)^{5/2}\frac{(\sigma_e)_{nf}}{(\sigma_e)_f}\frac{M}{(n+1)}f'^2\right]=0 \qquad \text{... (12)}$$

subjected to the relevant boundary conditions in the dimensionless form are

$$\begin{aligned}&\eta=0:\quad f=0,\ f'=1,\ \theta=1\\&\eta\to\infty:\quad f'\to0,\ \theta\to0\end{aligned} \qquad \text{... (13)}$$

where prime $(')$ represents the differentiation with respect to η, $M=\frac{(\sigma_e)_f\upsilon_f B_0{}^2\,\mathrm{Re}_x}{\rho_f u_w{}^2}$ is the magnetic parameter, $\mathrm{Re}_x=\frac{u_w x}{\upsilon_f}$ is the local Reynolds number, $\mathrm{Pr}=\frac{\upsilon_f}{\alpha_f}$ is the Prandtl number, $Br=\mathrm{Pr}\,Ec$ is the Brinkmann number and $Ec=\frac{u_w{}^2}{(C_p)_f(T_w-T_\infty)}$ is the Eckert number.

4 Quantities of Interest

Physical quantities in the vicinity of surface are the local skin friction coefficient C_f and the local Nusselt number Nu_x, which are expressed as

$$C_f=\frac{\tau_w}{\frac{\rho_f u_w{}^2}{2}},\quad Nu_x=\frac{xq_w}{\kappa_f(T_w-T_\infty)} \qquad \text{... (14)}$$

where $\tau_w=\mu_{nf}\left(\frac{\partial u}{\partial y}\right)_{y=0}$ and $q_w=-\kappa_{nf}\left(\frac{\partial T}{\partial y}\right)_{y=0}$ are the wall shear stress and the wall heat flux, respectively.

By using the dimensionless variables Eq. (10), the physical quantities Eq. (14) can be defined in the dimensional form as

$$Re_x^{1/2} C_f = \frac{1}{(1-\phi)^{5/2}} [2(n+1)]^{1/2} f''(0),$$

$$\frac{1}{Re_x^{1/2}} Nu_x = -\frac{\kappa_{nf}}{\kappa_f} \left(\frac{n+1}{2} \right)^{1/2} \theta'(0) \quad \ldots (15)$$

5 Computational Algorithm

Nonlinear ordinary differential Eqs. (11) and (12) along with the corresponding boundary conditions Eq. (13) are solved numerically by applying the Keller-Box method. For the computational process, the far-field boundary condition is considered a finite value as $\eta \to \infty = 6$.

5.1 Scheme of implicit finite difference

To reduce the Eqs. (11) and (12) into the first-order form, introducing the new dependent variables

$$f' = p \quad \ldots (16)$$

$$p' = q \quad \ldots (17)$$

$$\theta' = s \quad \ldots (18)$$

so the Eqs. (11) and (12) can be defined as

$$q' + (1-\phi)^{5/2} \left(1-\phi+\phi \frac{\rho_s}{\rho_f} \right) \left(fq - \frac{2n}{n+1} p^2 \right) - 2(1-\phi)^{5/2} \frac{(\sigma_e)_{nf}}{(\sigma_e)_f} \frac{M}{(n+1)} p = 0 \quad \ldots (19)$$

$$\frac{\kappa_{nf}}{\kappa_f} s' + \left[1-\phi+\phi \frac{(\rho C_p)_s}{(\rho C_p)_f} \right] Pr \left(fs - \frac{4n}{n+1} p\theta \right) + \frac{1}{(1-\phi)^{5/2}} Br \left[q^2 + 2(1-\phi)^{5/2} \frac{(\sigma_e)_{nf}}{(\sigma_e)_f} \frac{M}{(n+1)} p^2 \right] = 0 \quad \ldots (20)$$

with the corresponding boundary conditions Eq. (13) become

$$\eta = 0: \quad f = 0,\ p = 1,\ \theta = 1$$
$$\eta \to \infty: \quad p \to 0,\ \theta \to 0 \quad \ldots (21)$$

The rectangular grid $X\eta$ – plane and the net points are represented in Fig. 2 such as

$$x_0 = 0,\ x_i = x_{i-1} + k_i,\ i = 1,2,3,....I$$
$$\eta_0 = 0,\ \eta_j = \eta_{j-1} + h_j,\ j = 1,2,3,....J \quad \ldots (22)$$

For the mid point $\left(x_i, \eta_{j-\frac{1}{2}} \right)$ of the wedge BC, the Eqs. (16) to (20) are written in the finite difference form by using centered difference derivatives as

$$f_j - f_{j-1} - \frac{h_j}{2}(p_j + p_{j-1}) = 0 \quad \ldots (23)$$

$$p_j - p_{j-1} - \frac{h_j}{2}(q_j + q_{j-1}) = 0 \quad \ldots (24)$$

$$\theta_j - \theta_{j-1} - \frac{h_j}{2}(s_j + s_{j-1}) = 0 \quad \ldots (25)$$

$$\frac{1}{h_j}(q_j - q_{j-1}) + \frac{1}{4}(1-\phi)^{5/2} \left(1-\phi+\phi \frac{\rho_s}{\rho_f} \right) \left[(f_j + f_{j-1})(q_j + q_{j-1}) - \frac{2n}{n+1}(p_j + p_{j-1})^2 \right] - (1-\phi)^{5/2} \frac{(\sigma_e)_{nf}}{(\sigma_e)_f} \frac{M}{(n+1)} (p_j + p_{j-1}) = 0 \quad \ldots (26)$$

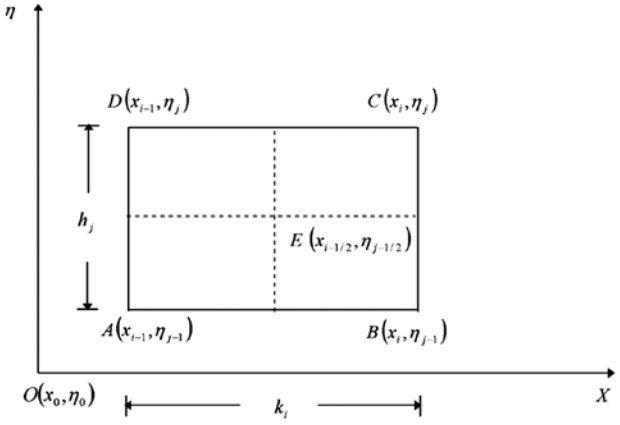

Fig. 2 — Net rectangle for difference approximation.

$$\frac{1}{h_j}\frac{\kappa_{nf}}{\kappa_f}\left(s_j - s_{j-1}\right)+\frac{1}{4}\left[1-\phi+\phi\frac{\left(\rho C_p\right)_s}{\left(\rho C_p\right)_f}\right]$$
$$Pr\left[\left(f_j + f_{j-1}\right)\left(s_j + s_{j-1}\right)-\frac{4n}{n+1}\left(p_j + p_{j-1}\right)\left(\theta_j + \theta_{j-1}\right)\right]$$
$$+\frac{1}{4}\frac{1}{(1-\phi)^{5/2}}$$
$$Br\left[\left(q_j + q_{j-1}\right)^2 + 2(1-\phi)^{5/2}\frac{\left(\sigma_e\right)_{nf}}{\left(\sigma_e\right)_f}\frac{M}{(n+1)}\left(p_j + p_{j-1}\right)^2\right] = 0 \quad \ldots (27)$$

Equations (23) to (27) are represented for $j = 1, 2, 3, \ldots . J-1$ and from the corresponding boundary conditions Eq. (21), at the initial condition $j = 0$ and far field condition $j = J$ it is given that

$$f_0 = 0, \quad p_0 = 1, \quad \theta_0 = 1, \quad p_J \to 0, \quad \theta_J \to 0 \quad \ldots (28)$$

5.2 Newton's method

Method of Newton is applied to convert the nonlinear system into a linear system. Some following iterations are introduce:

$$f_j^{(i+1)} = f_j^{(i)} + \delta f_j^{(i)},\ p_j^{(i+1)} = p_j^{(i)} + \delta p_j^{(i)},\ q_j^{(i+1)} = q_j^{(i)} + \delta q_j^{(i)},\ \theta_j^{(i+1)} = \theta_j^{(i)} + \delta\theta_j^{(i)},\ s_j^{(i+1)} = s_j^{(i)} + \delta s_j^{(i)} \quad \ldots (29)$$

The above expressions are substituting into the Eqs. (23) to (27) and then neglect the quadratic and successive order terms in $\delta f_j^{(i)}$, $\delta p_j^{(i)}$, $\delta q_j^{(i)}$, $\delta\theta_j^{(i)}$ and $\delta s_j^{(i)}$. So above expressions yields a tridiagonal structure as:

$$\delta f_j - \delta f_{j-1} - \frac{h_j}{2}(\delta p_j + \delta p_{j-1}) = (r_1)_{j-\frac{1}{2}} \quad \ldots (30)$$

$$\delta p_j - \delta p_{j-1} - \frac{h_j}{2}(\delta q_j + \delta q_{j-1}) = (r_2)_{j-\frac{1}{2}} \quad \ldots (31)$$

$$\delta\theta_j - \delta\theta_{j-1} - \frac{h_j}{2}(\delta s_j + \delta s_{j-1}) = (r_3)_{j-\frac{1}{2}} \quad \ldots (32)$$

$$(a_1)_{j-\frac{1}{2}}\delta f_j + (a_2)_{j-\frac{1}{2}}\delta f_{j-1} + (a_3)_{j-\frac{1}{2}}\delta p_j + (a_4)_{j-\frac{1}{2}}\delta p_{j-1} + (a_5)_{j-\frac{1}{2}}\delta q_j + (a_6)_{j-\frac{1}{2}}\delta q_{j-1} = (r_4)_{j-\frac{1}{2}} \quad \ldots (33)$$

$$(b_1)_{j-\frac{1}{2}}\delta f_j + (b_2)_{j-\frac{1}{2}}\delta f_{j-1} + (b_3)_{j-\frac{1}{2}}\delta p_j + (b_4)_{j-\frac{1}{2}}\delta p_{j-1} + (b_5)_{j-\frac{1}{2}}\delta q_j + (b_6)_{j-\frac{1}{2}}\delta q_{j-1} + (b_7)_{j-\frac{1}{2}}\delta\theta_j + (b_8)_{j-\frac{1}{2}}\delta\theta_{j-1} + (b_9)_{j-\frac{1}{2}}\delta s_j + (b_{10})_{j-\frac{1}{2}}\delta s_{j-1} = (r_5)_{j-\frac{1}{2}} \quad \ldots (34)$$

where,

$$(a_1)_{j-\frac{1}{2}} = (a_2)_{j-\frac{1}{2}} = \frac{1}{4}(1-\phi)^{5/2}\left(1-\phi+\phi\frac{\rho_s}{\rho_f}\right)(q_j + q_{j-1}),$$

$$(a_3)_{j-\frac{1}{2}} = (a_4)_{j-\frac{1}{2}} = -\frac{1}{4}(1-\phi)^{5/2}\left(1-\phi+\phi\frac{\rho_s}{\rho_f}\right)\frac{2n}{(n+1)}(p_j + p_{j-1}) - (1-\phi)^{5/2}\frac{(\sigma_e)_{nf}}{(\sigma_e)_f}\frac{M}{(n+1)},$$

$$(a_5)_{j-\frac{1}{2}} = \frac{1}{h_j} + \frac{1}{4}(1-\phi)^{5/2}\left(1-\phi+\phi\frac{\rho_s}{\rho_f}\right)(f_j + f_{j-1}),$$

$$(a_6)_{j-\frac{1}{2}} = -\frac{1}{h_j} + \frac{1}{4}(1-\phi)^{5/2}\left(1-\phi+\phi\frac{\rho_s}{\rho_f}\right)(f_j + f_{j-1}),$$

$$(b_1)_{j-\frac{1}{2}} = (b_2)_{j-\frac{1}{2}} = \frac{1}{4}\left[1-\phi+\phi\frac{\left(\rho C_p\right)_s}{\left(\rho C_p\right)_f}\right]Pr(s_j + s_{j-1}),$$

$$(b_3)_{j-\frac{1}{2}} = (b_4)_{j-\frac{1}{2}} = -\left[1-\phi+\phi\frac{\left(\rho C_p\right)_s}{\left(\rho C_p\right)_f}\right]\frac{n\,Pr}{n+1}(\theta_j + \theta_{j-1}) + \frac{1}{2}\frac{\left(\sigma_e\right)_{nf}}{\left(\sigma_e\right)_f}\frac{M\,Br}{n+1}(p_j + p_{j-1}),$$

$$(b_5)_{j-\frac{1}{2}} = (b_6)_{j-\frac{1}{2}} = \frac{1}{4}\frac{1}{(1-\phi)^{5/2}}Br\,(q_j + q_{j-1}),$$

$$(b_7)_{j-\frac{1}{2}} = (b_8)_{j-\frac{1}{2}} = -\left[1-\phi+\phi\frac{(\rho C_p)_s}{(\rho C_p)_f}\right]\frac{n\,Pr}{n+1}(p_j + p_{j-1}),$$

$$(b_9)_{j-\frac{1}{2}} = \frac{1}{h_j}\frac{\kappa_{nf}}{\kappa_f} + \frac{1}{4}\left[1-\phi+\phi\frac{(\rho C_p)_s}{(\rho C_p)_f}\right]\Pr(f_j + f_{j-1}),$$

$$(b_{10})_{j-\frac{1}{2}} = -\frac{1}{h_j}\frac{\kappa_{nf}}{\kappa_f} + \frac{1}{4}\left[1-\phi+\phi\frac{(\rho C_p)_s}{(\rho C_p)_f}\right]\Pr(f_j + f_{j-1}),$$

$$(r_1)_{j-\frac{1}{2}} = -(f_j - f_{j-1}) + \frac{h_j}{2}(p_j + p_{j-1}),$$

$$(r_2)_{j-\frac{1}{2}} = -(p_j - p_{j-1}) + \frac{h_j}{2}(q_j + q_{j-1}),$$

$$(r_3)_{j-\frac{1}{2}} = -(\theta_j - \theta_{j-1}) + \frac{h_j}{2}(s_j + s_{j-1}),$$

$$(r_4)_{j-\frac{1}{2}} = -\frac{1}{h_j}(q_j - q_{j-1}) - \frac{1}{4}(1-\phi)^{5/2}\left(1-\phi+\phi\frac{\rho_s}{\rho_f}\right)\left[(f_j + f_{j-1})(q_j + q_{j-1}) - \frac{2n}{n+1}(p_j + p_{j-1})^2\right] + (1-\phi)^{5/2}\frac{(\sigma_e)_{nf}}{(\sigma_e)_f}\frac{M}{(n+1)}(p_j + p_{j-1}),$$

$$(r_5)_{j-\frac{1}{2}} = -\frac{1}{h_j}\frac{\kappa_{nf}}{\kappa_f}(s_j - s_{j-1}) - \frac{1}{4}\left[1-\phi+\phi\frac{(\rho C_p)_s}{(\rho C_p)_f}\right]Pr\left[(f_j + f_{j-1})(s_j + s_{j-1}) - \frac{4n}{n+1}(p_j + p_{j-1})(\theta_j + \theta_{j-1})\right] - \frac{1}{4}\frac{1}{(1-\phi)^{5/2}}Br\left[(q_j + q_{j-1})^2 + 2(1-\phi)^{5/2}\frac{(\sigma_e)_{nf}}{(\sigma_e)_f}\frac{M}{(n+1)}(p_j + p_{j-1})^2\right]$$

For all iterates, it is assumed as

$$\delta f_0 = 0, \quad \delta p_0 = 0, \quad \delta\theta_0 = 0, \ \delta p_J = 0, \ \delta\theta_J = 0 \qquad \ldots (35)$$

5.3 Block elimination method

Equations (30) to (34) are writing in the block tridiagonal matrix form.

$$\begin{bmatrix} [A_1] & [C_1] & & & \\ [B_2] & [A_2] & [C_2] & & \\ & & \ddots & \cdots & \\ & & & [B_{J-1}] & [A_{J-1}] & [C_{J-1}] \\ & & & & [B_J] & [A_J] \end{bmatrix} \begin{bmatrix} [\delta_1] \\ [\delta_2] \\ \vdots \\ [\delta_{J-1}] \\ [\delta_J] \end{bmatrix} = \begin{bmatrix} [r_1] \\ [r_2] \\ \vdots \\ [r_{J-1}] \\ [r_J] \end{bmatrix}$$

that is,

$$[A][\delta] = [r] \qquad \ldots (36)$$

where the elements are,

$$[A_1] = \begin{bmatrix} 0 & 0 & 1 & 0 & 0 \\ \frac{-h_j}{2} & 0 & 0 & \frac{-h_j}{2} & 0 \\ 0 & \frac{-h_j}{2} & 0 & 0 & \frac{-h_j}{2} \\ a_6 & 0 & a_1 & a_5 & 0 \\ b_6 & b_{10} & b_1 & b_5 & b_9 \end{bmatrix},$$

$$[A_j] = \begin{bmatrix} \frac{-h_j}{2} & 0 & 1 & 0 & 0 \\ -1 & 0 & 0 & \frac{-h_j}{2} & 0 \\ 0 & -1 & 0 & 0 & \frac{-h_j}{2} \\ a_4 & 0 & a_1 & a_5 & 0 \\ b_4 & b_8 & b_1 & b_5 & b_9 \end{bmatrix} \quad for\ 2 \le j \le J,$$

$$[B_j] = \begin{bmatrix} 0 & 0 & -1 & 0 & 0 \\ 0 & 0 & 0 & \frac{-h_j}{2} & 0 \\ 0 & 0 & 0 & 0 & \frac{-h_j}{2} \\ 0 & 0 & a_2 & a_6 & 0 \\ 0 & 0 & b_2 & b_6 & b_{10} \end{bmatrix} for 2 \le j \le J,$$

$$[C_j] = \begin{bmatrix} \frac{-h_j}{2} & 0 & 0 & 0 & 0 \\ 1 & 0 & 0 & 0 & 0 \\ 0 & 1 & 0 & 0 & 0 \\ a_3 & 0 & 0 & 0 & 0 \\ b_3 & b_7 & 0 & 0 & 0 \end{bmatrix} for 1 \le j \le J-1,$$

$$[\delta_1]=\begin{bmatrix}\delta q_0\\ \delta s_0\\ \delta f_1\\ \delta q_1\\ \delta s_1\end{bmatrix}, [\delta_j]=\begin{bmatrix}\delta p_{j-1}\\ \delta \theta_{j-1}\\ \delta f_j\\ \delta q_j\\ \delta s_j\end{bmatrix} \text{ for } 2\le j\le J$$

and

$$[r_j]=\begin{bmatrix}(r_1)_j\\ (r_2)_j\\ (r_3)_j\\ (r_4)_j\\ (r_5)_j\end{bmatrix} \text{ for } 1\le j\le J.$$

Forward sweep: Matrix A is surmised as a nonsingular matrix to found the solution of the Eq. (36) then the matrix A can be taken as:

$$[A]=[L][U] \quad \text{... (37)}$$

$$[L]=\begin{bmatrix}[\alpha_1] & & & & \\ [B_2] & [\alpha_2] & & & \\ & \ddots & & & \\ & & & [\alpha_{J-1}] & \\ & & & [B_J] & [\alpha_J]\end{bmatrix} \quad \text{and}$$

$$[U]=\begin{bmatrix}I & [\beta_1] & & & \\ & I & [\beta_2] & & \\ & & \ddots & \ddots & \\ & & & I & [\beta_{J-1}]\\ & & & & I\end{bmatrix}$$

Where, I is the identity matrix of order 5×5, and $[\alpha_j]$ and $[\beta_j]$ are the matrix of order 5×5. Elements of these matrices are found by the following relations:

$$[\alpha_1]=[A_1] \quad \text{... (38)}$$

$$[A_1][\beta_1]=[C_1] \quad \text{... (39)}$$

$$[\alpha_j]=[A_j]-[B_j][\beta_{j-1}],\ \ j=2,3,....J \quad \text{... (40)}$$

Backward sweep:

In view of,

$$[L][U][\delta_j]=[r_j] \quad \text{... (41)}$$

with the consideration as:

$$[U][\delta_j]=[W_j] \quad \text{... (42)}$$

$$[L][W_j]=[r_j] \quad \text{... (43)}$$

where $[W_j]$ are the column matrix of order 5×1 and elements of $[W_j]$ can be determined from Eq. (43) as:

$$[\alpha_1][W_1]=[r_1] \quad \text{... (44)}$$

$$[\alpha_j][W_j]=[r_j]-[B_j][W_{j-1}],\ \ 2\le j\le J \quad \text{... (45)}$$

A step in which $[\alpha_j]$, $[\beta_j]$ and $[W_j]$ are found in commonly known as the forward sweep. While once the elements of $[W_j]$ are predicted, the Eq. (42) commits the solution known as backward sweep, whose elements can be obtained by the given relations

$$[\delta_j]=[W_j]-[\beta_j][\delta_{j+1}],\ \ 1\le j\le J-1 \quad \text{... (46)}$$

$$[\delta_J]=[W_J] \quad \text{... (47)}$$

These iterative procedures are repeated until convergence rule is satisfied with maintaining accuracy of 10^{-7} and process are stopped when $\left|\delta q_0^{(i)}\right|\le\xi$, where ξ is a small prescribed value.

6 Results Validation

The accuracy of the results is necessary to check the validation of the proposed method. So current data are compared with the previously published data as Hamad and Ferdows[39] for the impacts of the various types of nanofluids, the solid volume fraction ϕ and the Eckert number Ec. An outstanding correspondence can be seen between the present data and the earlier published data as revealed in Table 2.

Table 2 — Comparison of numerical values of $f''(0)$ and $\theta'(0)$ for different types of nanofluids and several values of ϕ and Ec with $n = 10.0$, $M = 0.0$ and $Pr = 10.0$.

Nanofluids	ϕ	Ec	$-f''(0)$		$-\theta'(0)$	
			Hamad and Ferdows[39]	Present results	Hamad and Ferdows[39]	Present results
Cu – water	0.05	0.0	1.40049	1.3695799	5.62189	5.6327626
		0.1			5.36853	5.3965271
	0.10	0.0	1.47769	1.4508113	5.17237	5.1824429
		0.1			4.88417	4.9110821
	0.15	0.0	1.51794	1.4929180	4.77257	4.7825143
		0.1			4.45581	4.4831142
	0.20	0.0	1.52880	1.5042506	4.41306	4.4233088
		0.1			4.07241	4.1012914
Ag – water	0.05	0.0	1.43646	1.4075115	5.57754	5.5878689
		0.1			5.31281	5.3396891
	0.10	0.0	1.53712	1.5129208	5.09104	5.1003678
		0.1			4.78234	4.8076156
	0.15	0.0	1.59300	1.5710410	4.65991	4.6690030
		0.1			4.31513	4.3404715
	0.20	0.0	1.61399	1.5928105	4.27371	4.2830432
		0.1			3.89874	3.9253718

7 Graphical Results and Discussion

The natures of the velocity and the temperature profiles for different kinds of nanofluids and involved controlling parameters such as the solid volume fraction ϕ, the nonlinear stretching parameter n, the magnetic parameter M and the Brinkmann number Br along to $Cu-$water nanofluid are addressed via graphically. Further, the behaviors of the wall shear stress and the wall heat flux for various types of nanofluids and for several values of considering parameters with $Cu-$water nanofluid are presented in tabular form and discussed in an extensive way. Due to find the effect of anyone specified parameter on the velocity field, the temperature field, the local skin friction coefficient and the local Nusselt number, all remaining parameters are taken as constant.

Figures 3 and 4 portray to indicate the reaction of the several types of nanoparticles, namely Ag, Cu, TiO_2 and Al_2O_3 along to the base fluid water on the velocity $f'(\eta)$ and the temperature $\theta(\eta)$ distributions respectively. From these figures, it can be observed that the momentum boundary layer enhances for the increasing manner of nanoparticles sequence such as Ag, Cu, TiO_2 and Al_2O_3 with the water base fluid, while opposite effect is found in the thermal boundary layer for the sequence of the nanoparticles as Ag, Cu, Al_2O_3 and TiO_2 along to the base fluid water. This happens because different

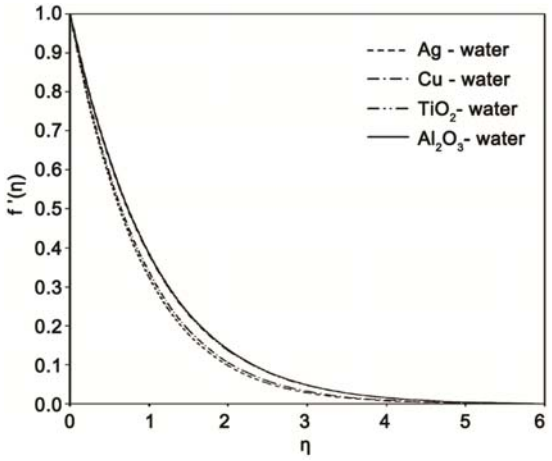

Fig. 3 — Plots of velocity fields for various types of nanofluids with $\phi = 0.07$, $n = 0.5$ and $M = 0.01$.

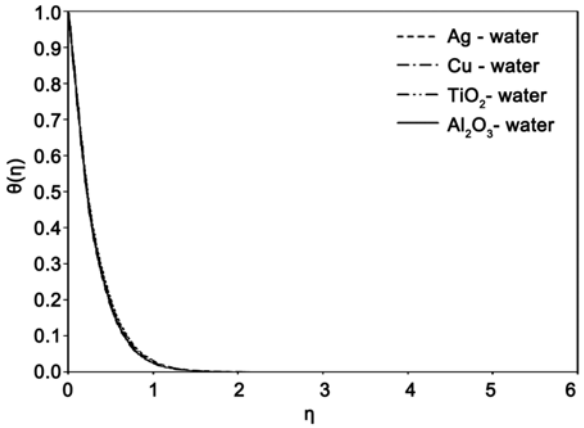

Fig. 4 — Plots of temperature fields for various types of nanofluids with $\phi = 0.07$, $n = 0.5$, $M = 0.01$, $Pr = 6.8$ and $Br = 0.1$.

types of materials have distinct mechanical and physical characteristics. So the velocity and the temperature fields change along to the change of type of solid nanoparticles in the water-based fluid.

Behaviors of the dimensionless velocity $f'(\eta)$ and the dimensionless temperature $\theta(\eta)$ for the effect of ϕ are given through Figs (5 and 6), respectively. It can be noted from these figures that enlargement in ϕ leads to decline the fluid flow and fluid temperature grows-up. This may attribute to the reason that suspended nanoparticles have increasing nature resistance flow, which reduces the velocity field. Moreover, for the rising values of the solid volume fraction, the thermal conductivity of nanofluid develops which leads the enhancement in the thermal boundary layer.

Figures 7 and 8 show the impact of n on the fluid flow $f'(\eta)$ and the temperature $\theta(\eta)$ respectively. It can be seen that the momentum boundary layer as well as the fluid temperature step-down when n rises. Physically it occurs because the ratio of the stretching velocity to the external stream velocity is known as the stretching parameter. Therefore, for an increment in the stretching parameter, stretching velocity controls the external stream velocity, which leads to

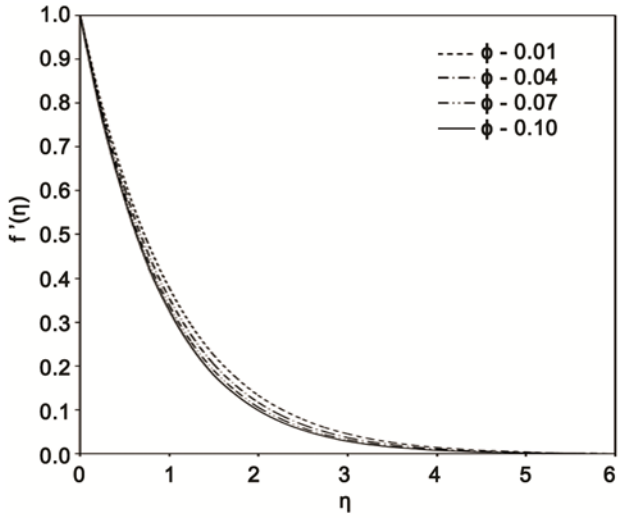

Fig. 5 — Plots of velocity fields for various values of ϕ with $n = 0.5$ and $M = 0.01$ over Cu – water nanofluid.

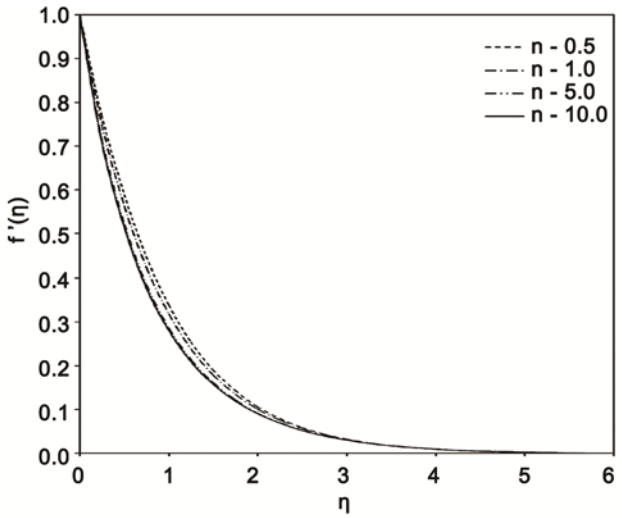

Fig. 7 — Plots of velocity fields for various values of n with $\phi = 0.07$ and $M = 0.01$ over Cu – water nanofluid.

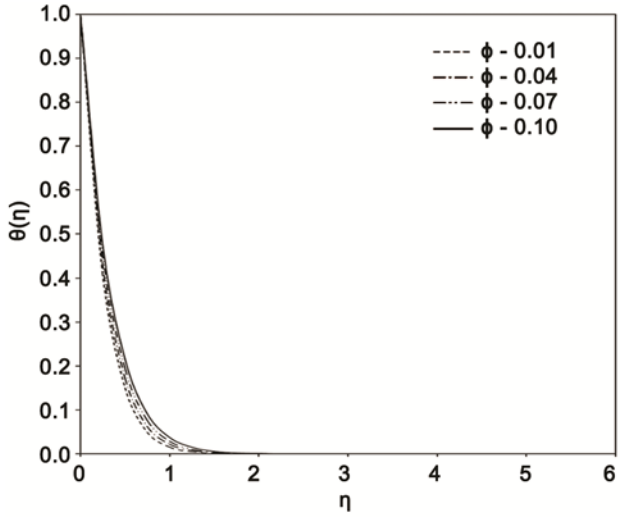

Fig. 6 — Plots of temperature fields for various values of ϕ with $n = 0.5$, $M = 0.01$, $Pr = 6.8$ and $Br = 0.1$ over Cu – water nanofluid.

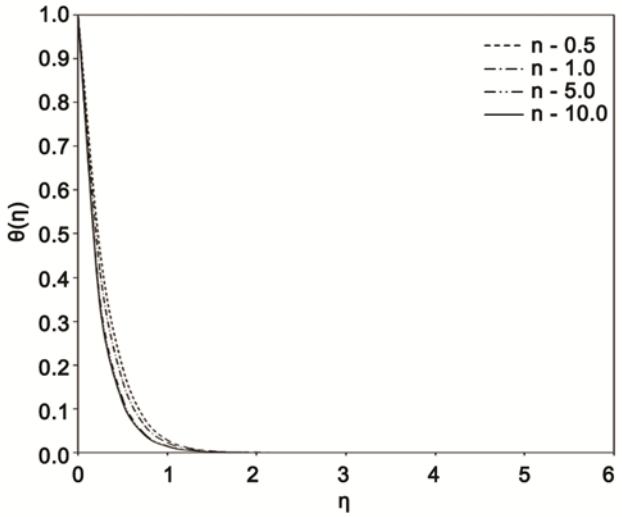

Fig. 8 — Plots of temperature fields for various values of n with $\phi = 0.07$, $M = 0.01$, $Pr = 6.8$ and $Br = 0.1$ over Cu – water nanofluid.

decline the thickness of the momentum boundary layer and the thermal boundary layer.

Impacts of M on the velocity $f'(\eta)$ and the temperature $\theta(\eta)$ fields are plotted in Figs 9 and 10, respectively. It is interesting to note that the velocity of fluid reduces with development in M, although the reverse effect can be seen in the temperature. From a physical point of view, a drag like force as Lorentz force yields for the greater value of the magnetic parameter. Lorentz force leads the development to the motion of fluid resistive and creates more resulting heat in enlargement of the thermal boundary layer.

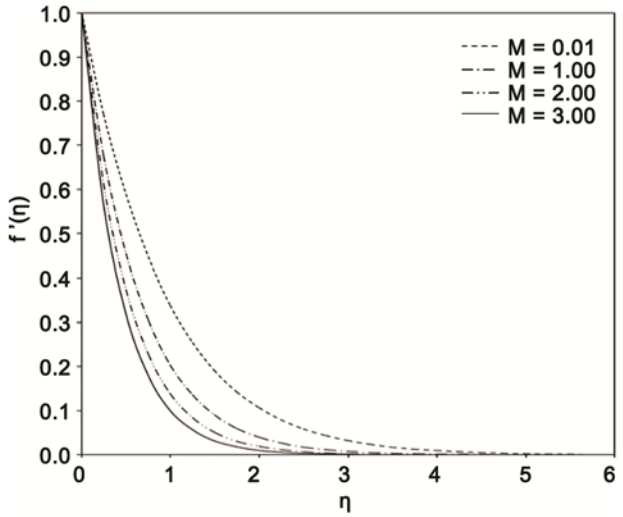

Fig. 9 — Plots of velocity fields for various values of M with $\phi = 0.07$ and $n = 0.5$ over Cu – water nanofluid.

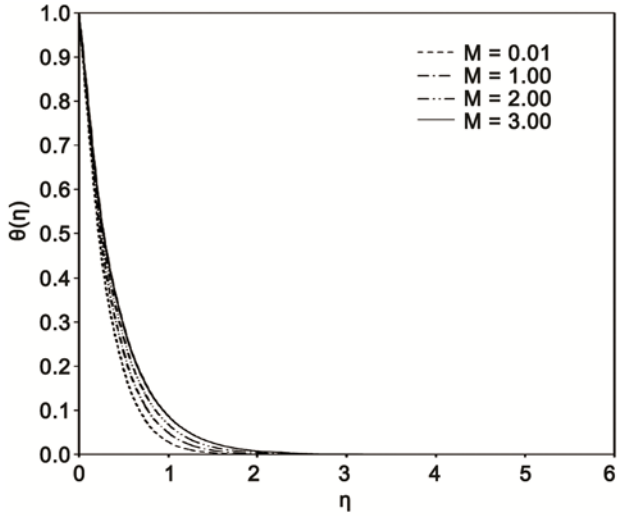

Fig. 10 — Plots of temperature fields for various values of M with $\phi = 0.07$, $n = 0.5$, $Pr = 6.8$ and $Br = 0.1$ over Cu – water nanofluid.

Figure 11 displays the nature of the temperature $\theta(\eta)$ for changing values of Br. From this figure, it is observed that the temperature distribution increases smoothly with the rising values of Br. This happens with the critical fact that the influence of viscous dissipation on the area of flow is to develop the energy, which creates buoyancy force and the higher temperature field. Along with the rising dissipation parameter, an increment in the buoyancy force leads the fluid temperature to rise.

Table 3 indicates the impacts of the various types of nanofluids and the influences of ϕ, n, M and Br along to Cu – water nanofluid on the surface shear stress $f''(0)$ and the surface heat flux $\theta'(0)$. It can be seen from Eq. (15) that the surface shear stress $f''(0)$ and the rate of heat transfer $\theta'(0)$ are proportional to the local skin friction coefficient C_f and the local Nusselt number Nu_x respectively. This table exhibits that the local skin friction coefficient develops by the increasing sequence of nanoparticles such as Ag, Cu, TiO_2 and Al_2O_3 along to the conventional fluid water, while the local Nusselt number depreciates via the rising order of solid nanoparticles namely Ag, Cu, Al_2O_3 and TiO_2 with the base fluid water. Subsequently, it is noted that the wall heat flux as well as the heat transfer rate decline with the development in ϕ, n and M, although the reverse effect is found in rate of heat transfer for the

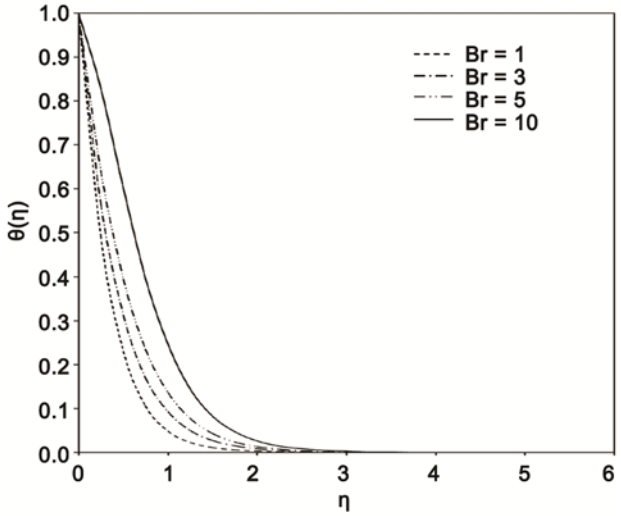

Fig. 11 — Plots of temperature fields for various values of Br with $\phi = 0.07$, $n = 0.5$, $M = 0.01$ and $Pr = 6.8$ over Cu – water nanofluid.

Table 3 — Numerical data of $f''(0)$ and $\theta'(0)$ for distinct types of nanofluids and several values of considering parameters with $Pr = 6.8$.

Nanofluids	ϕ	n	M	Br	$-f''(0)$	$-\theta'(0)$
Ag – water	0.07	0.5	0.01	0.1	1.0555077	2.9002370
Cu – water					1.0205750	2.9380805
TiO_2 – water					0.9082814	3.0141410
Al_2O_3 – water					0.9011290	2.9759800
Cu – water	0.01				0.9203500	3.2801935
	0.04				0.9777015	3.1018390
	0.10				1.0515830	2.7868846
	0.07	1.0			1.1443318	3.4219810
		5.0			1.3627349	4.2353701
		10.0			1.4081536	4.4000500
		0.5	1.00		1.5428459	2.7568148
			2.00		1.9341546	2.6157980
			3.00		2.2589790	2.4964190
			0.01	1.0	1.0205750	2.7071960
				3.0		2.1941205
				5.0		1.6810447
				10.0		0.3983550

enhancing value of ϕ and M. It is also observed from this table that increasing nature of Br tends to the increment in the local Nusselt number. Further, for all values of the considering parameters, the negative value of shear stress denotes that fluid exerts a drag force by the wall and negative value of heat flux indicates that there is a heat flow on the wall.

8 Conclusions

In the present article, the viscous dissipation and Joule heating influences on MHD boundary layer flow of nanofluids due to a nonlinear stretchable surface are discussed. Convenient similarity variables are introduced to convert the set of partial differential equations into the system of ordinary differential equations. Keller-box method is applied to find the solutions of transformed equations. An investigation is made via the graphical and tabulated data for the effects of physical parameters. This analysis reveals the following main findings

(i) The momentum boundary layer and the surface shear stress are lower for Ag nanoparticles along to the base fluid water, while Al_2O_3 nanoparticles with the base fluid water have greater momentum boundary layer and the surface shear stress as compared to the other solid nanoparticles Cu and TiO_2 along to the conventional fluid water. Moreover, mixture of Ag nanoparticles and the ordinary fluid water has higher development in the temperature of the fluid and the heat flux than remaining nanofluids.

(ii) Enhancing values of the solid volume fraction, the nonlinear stretching parameter and the magnetic parameter lead to the decreasing nature of the dimensionless velocity, the dimensionless temperature, the local skin friction and the local Nusselt number, while reverse phenomenon occurs in the fluid temperature and the surface heat flux for the rising values of the solid volume fraction and the magnetic parameter.

(iii) Effects of evolving values of the Brinkmann number is directed towards to cause the increment in the temperature field as well as the local Nusselt number.

Nomenclature

b, c	positive constants
$\vec{B}$	transverse magnetic field $\left(Nm^{-1}A^{-1}\right)$
B_0	magnetic field strength $\left(Nm^{-1}A^{-1}\right)$
Br	Brinkmann number
C_f	local skin friction coefficient
C_p	specific heat at constant pressure $\left(JKg^{-1}K^{-1}\right)$

Ec	Eckert number
f	dimensionless stream function
$\vec{J}$	electric current density $\left(Am^{-2}\right)$
M	magnetic parameter
n	nonlinear stretching parameter
Nu_x	local Nusselt number
Pr	Prandtl number
q_w	surface heat flux $\left(Wm^{-2}\right)$
Re_x	local Reynolds number
T	temperature of nanofluid (K)
T_w	fluid temperature at the surface (K)
T_∞	ambient fluid temperature (K)
u	velocity component corresponding to the $x-$axis $\left(ms^{-1}\right)$
u_w	nonlinear velocity at the surface $\left(ms^{-1}\right)$
v	velocity component corresponding to the $y-$axis $\left(ms^{-1}\right)$
x	direction parallel to the plate (m)
y	direction perpendicular to the plate (m)

Greek symbols

α	thermal diffusivity $\left(m^2s^{-1}\right)$
η	similarity variable
θ	dimensionless temperature
κ	thermal conductivity $\left(Wm^{-1}K^{-1}\right)$
μ	coefficient of viscosity $\left(Kgm^{-1}s^{-1}\right)$
υ	kinematic viscosity $\left(m^2s^{-1}\right)$
ρ	density $\left(Kgm^{-3}\right)$
σ_e	electric conductivity $\left(Sm^{-1}\right)$
τ_w	surface shear stress $\left(Nm^{-2}\right)$
ϕ	solid volume fraction
ψ	stream function $\left(m^2s^{-1}\right)$

Superscripts

$'$	differentiation with respect to η

Subscripts

f	base fluid
nf	nanofluid
s	nano solid particles

References

1 Yan W M, *Int J Heat Mass Transf*, 38 (1995) 2101.
2 Datta A K, *J Food Eng*, 39 (1999) 285.
3 Khanafer K, Vafai K & Lightstone M, *Int J Heat Mass Transf*, 46 (2003) 3639.
4 Wang C H & Yang R, *Appl Math Comput*, 173 (2006) 1246.
5 Hong C & Asako Y, *Appl Therm Eng*, 28 (2008) 1375.
6 Yan B H & Gu H Y, *Ann Nucl Energy*, 38 (2011) 1833.
7 Turkyilmazoglu M, *Comput Fluids*, 94 (2014) 139.
8 Chaudhary S & Choudhary M K, *Indian J Pure Appl Phys*, 54 (2016) 209.
9 Zhang Y, Zhao H J & Bai Y, *Commun Theor Phys*, 67 (2017) 697.
10 Afridi M I & Qasim M, *Int J Therm Sci*, 123 (2018) 117.
11 Hayat T, Hutter K, Asghar S & Siddiqui A M, *Math Comput Model*, 36 (2002) 987.
12 Siddheshwar P G & Mahabaleswar U S, *Int J Non-Linear Mech*, 40 (2005) 807.
13 Abdelkhalek M M, *Comp Mater Sci*, 43 (2008) 384.
14 Turkyilmazoglu M, *Int J Therm Sci*, 50 (2011) 88.
15 Chaudhary S & Kumar P, *Meccanica*, 49 (2014) 69.
16 Imtiaz M, Hayat T, Alsaedi A & Hobiny A, *J Mol Liq*, 221 (2016) 245.
17 Chaudhary S, Kanika K M & Choudhary M K, *Indian J Pure Appl Phys*, 56 (2018) 931.
18 Choi S U S, *Publ Fed*, 231ASME (1995) 99.
19 Eastman J A, Choi S U S, Li S, Yu W & Thompson L J, *Appl Phys Lett*, 78 (2001) 718.
20 Koo J & Kleinstreuer C, *Int J Heat Mass Transf*, 48 (2005) 2652.
21 Akbarinia A, *Int J Heat Fluid Flow*, 29 (2008) 229.
22 Rana P, Bhargava R & Beg O A, *Comput Math Appl*, 64 (2012) 2816.
23 Moghari R M, Talebi F, Rafee R & Shariat M, *Heat Transf Eng*, 36 (2015) 166.
24 Sheikholeslami M & Rokni H B, *Chinese J Phys*, 55 (2017) 1352.
25 Sheikholeslami M & Zeeshan A, *Int J Numer Methods Heat Fluid Flow*, 28 (2018) 641.
26 Nazar R, Amin N, Filip D & Pop I, *Int J Eng Sci*, 42 (2004) 1241.
27 Cortell R, *Appl Math Comput*, 184 (2007) 864.
28 Jat R N & Chaudhary S, *Z Angew Math Phys*, 61 (2010) 1151.
29 Cortell R, *Energy*, 74 (2014) 896.
30 Hayat T, Aziz A, Muhammad T, Alsaedi A & Mustafa M, *Adv Powder Technol,* 27 (2016) 1992.
31 Chaudhary S & Choudhary M K, *Therm Sci*, 22 (2018) 797.
32 Saadatmandi A & Sanatkar Z, *Appl Math Comput*, 323 (2018) 193.
33 El-Amin M F, *J Magn Magn Mater*, 263 (2003) 337.
34 Abo-Eldahab E M & El Aziz M A, *Appl Math Model*, 29 (2005) 579.
35 Jat R N & Chaudhary S, *Il Nuovo Cimento*, 124 B (2009) 53.
36 Reddy C R, Rao C V & Surender O, *Procedia Eng*, 127 (2015) 1219.

37 Hussain A, Malik M Y, Salahuddin T, Bilal S & Awais M, *J Mol Liq*, 231 (2017) 341.

38 Chaudhary S & Choudhary M K, *Eng Comput*, 35 (2018) 1675.

39 Hamad M A A & Ferdows M, *Appl Math Mech- Engl Ed*, 33 (2012) 923.

40 Bansal J L, Magnetohydrodynamics of viscous fluids, *Jaipur Pub House,* India (1994).

41 Mohyud-Din S T, Khan U & Hassan S M, *Adv Mech Eng*, 8 (2016) 1.

42 Su X & Zheng L, *Central Euro J Phys*, 11 (2013) 1694.